Arab J Sci Eng (2018) 43:2069–2081
https://doi.org/10.1007/s13369-017-2971-7

RESEARCH ARTICLE - CIVIL ENGINEERING

Basin Edge Effect on Seismic Ground Response: A Parametric Study for Duzce Basin Case, Turkey

Murat Emre Hasal[1] · **Recep Iyisan**[2] · **Hiroaki Yamanaka**[3]

Received: 22 March 2017 / Accepted: 8 November 2017 / Published online: 21 November 2017

Abstract In this study, edge effect on the spatial variation of surface ground motion was evaluated by conducting one (1D) and two-dimensional (2D) dynamic analyses on the numerical model of Duzce basin. Duzce is a province in northwestern Turkey and was hit by a devastating earthquake in November 1999. In order to estimate the seismic behavior of Duzce basin, 1D and 2D dynamic response analyses were carried out on its numerical model by using the seismic bedrock motion data derived from the deconvolution analysis of the N–S component of 1999 Duzce earthquake accelerogram. In addition, a series of different accelerograms and slope values were utilized to investigate the possible effects of change in strong ground motion intensity level and edge geometry on the dynamic response of soil layers over inclined bedrock. The finite element model for the edge section of the flat sedimentary basin was set up by using the 2D shear wave velocity profile, geotechnical and geological site conditions in Duzce. The variation of 2D/1D spectral acceleration ratios and aggravation factors with distance from basin edge was obtained for different period values. The results indicate that the aggravation factors reached their maximum values at a specific zone near basin edge and they generally converged to 1 regardless of the bedrock inclination or period values with increasing distance from the edge section. The highest aggravation factor values were calculated as 2.0–2.5 for the period interval of $T = 0.2$–0.6 s. A relationship was proposed between the aggravation factor and basin edge geometry.

Keywords Edge effect · Duzce basin · Amplification · 2D dynamic analysis · Aggravation factor

✉ Murat Emre Hasal
murat.hasal@bursa.bel.tr

Recep Iyisan
iyisan@itu.edu.tr

Hiroaki Yamanaka
yamanaka@depe.titech.ac.jp

[1] Department of Construction, Directorate of Projects, Bursa Metropolitan Municipality, Bursa, Turkey

[2] Civil Engineering Department, Faculty of Civil Engineering, Istanbul Technical University, Maslak 34469, Istanbul, Turkey

[3] Interdisciplinary Graduate School of Science and Engineering, Tokyo Institute of Technology, 4259, Nagatsuta-cho, Midori-ku, Yokohama 226-8502, Japan

List of symbols

1D	One dimensional
2D	Two dimensional
3D	Three dimensional
A	Soil amplification
ASI	Acceleration spectrum intensity
a_{max}	Peak ground acceleration
a_{max_r}	Maximum absolute acceleration of rock outcrop motion
a_{max_s}	Maximum absolute surface acceleration
a_{rms}	Root-mean-square of acceleration
CAV	Cumulative absolute velocity
D	Basin depth
d_{max}	Peak ground displacement
E–W	East–west
f_{max}	Maximum frequency of input motion
G	Shear modulus
H	Width of the inclined bedrock at basin edge
h	Finite element height
H/V	Horizontal/vertical
I_a	Arias intensity
l	Finite element length
LL	Liquid limit

M_d	Duration magnitude
M_L	Local magnitude
M_w	Moment magnitude
NAF	North Anatolian Fault
N–S	North–south
PI	Plasticity index
SMA	Sustained maximum acceleration
SPT-N	Standard penetration test blow count
$S(T)$[2D/1D]	Ratio of the spectral accelerations calculated from 2D and 1D dynamic analyses—aggravation factor
T	Period
TR	Turkey
USA	United States of America
VSI	Velocity spectrum intensity
v_{max}	Peak ground velocity
V_s	Shear wave velocity
X	The distance of a surface point from the beginning of rock outcrop at basin edge
α	Basin edge angle
γ_c	Cyclic shear strain
ξ	Damping ratio

1 Introduction

Evaluation of surface ground motion during earthquakes is one of the most challenging issues in geotechnical earthquake engineering. Severity and spatial distribution of ground motion is affected by geological and geotechnical conditions as well as earthquake source properties. During an earthquake excitation, local site conditions can have a strong effect on ground motion. The variation of seismic ground motion is denoted as amplification or deamplification of seismic waves at all frequencies. The fundamental cause for the amplification of motion over soft sediments is the seismic waves being trapped due to the impedance contrast between sediments and the underlying bedrock. Soil amplification depends on several parameters such as incoming wave properties, dynamic characteristics of soil layers, geometrical features like surface/subsurface topography and seismic bedrock depth [1]. At sites with topographical irregularities such as steep ridges and crests, formations with strong lateral geological discontinuities like narrow valleys and basins, two-dimensional (2D) and even three-dimensional (3D) dynamic effects may arise [2–6].

In the last decades, extensive instrumental seismic array observations were performed in the field in order to verify and validate the theoretical studies regarding basin effects. Some of the well-known observation sites can be given as the Ashigara Valley [7] and Ohba Valley [8] in Japan, the Parkway Valley in New Zealand [9], the Coachella Valley in southern California [10], the Volvi Basin in Greece [5,11–13], the Heathcote Valley in the Christchurch City of New Zealand [14].

Basin edge effect can be defined as the change in frequency content and intensity of earthquake ground motion due to seismic wave transformation and interference occurred at soil deposits laying over inclined bedrock near edge region [15,16]. This phenomenon depends mainly on the basin depth, edge bedrock inclination and geometry, dynamic properties of soil layers and characteristics of seismic bedrock ground motion [17–19].

In this study, the effect of the change in edge bedrock inclination on the seismic response behavior of a flat sedimentary basin was evaluated by performing 1D and 2D dynamic analyses using two-dimensional basin edge models. Basin models with different edge slope values were set up to determine the effects of edge inclination on the variation of surface motion under earthquake excitations with different frequency contents. Six separate input rock motions were used in the dynamic analyses to find out the effects of intensity and frequency content of bedrock earthquake motion on the basin models. For different sections of basin models, acceleration time histories and acceleration response spectra were obtained. Furthermore, the variations of the soil amplifications with the distance from the basin edges were investigated. 2D/1D spectral acceleration ratios which are known as aggravation factors were calculated, and the change in aggravation factor values with the distance from basin edges was examined for different period values in order to understand the difference between 1D and 2D dynamic behaviors. Next, the acceleration time histories and acceleration response spectra, which were obtained for different sections of the basin surface, were taken into consideration by a statistical approach and the relation between the results of 1D and 2D dynamic analyses was studied by calculating spectral acceleration ratios for different period values.

The shear wave velocity profile, geotechnical and geological site conditions in Duzce basin were used to build the two-dimensional finite element model of the basin edge. The deep shear wave velocity profile and depth of bedrock in Duzce basin were obtained from the microtremor array measurements by using the principle of accordance of H/V spectral ratio observed in single-point microtremor measurements with the ellipticity of theoretical Rayleigh wave [20].

2 Duzce Basin and Geotechnical Site Conditions

Duzce basin is located on the North Anatolian Fault (NAF) system which is known to be the most important fault system in Turkey. Throughout the history, many earthquakes had occurred in the vicinity of Duzce basin. Moreover, a devastating earthquake hit the city of Duzce on November 12, 1999, with a moment magnitude (M_w) of 7.2, causing heavy

damage and fatalities in Duzce Province. The 1999 Duzce earthquake occurred along the Duzce segment of North Anatolian Fault just a few months after the catastrophic August 17, 1999, Izmit (Kocaeli) earthquake [21]. Both the epicenters of these earthquakes and the relevant fault system are shown in Fig. 1.

Duzce basin and its surrounding area consist of alluvium deposits and lake sediments, which are composed of fine-grained gravel, sand and silt mixture with clay layers. While younger deposits of sediments are located in the center of basin, rock outcrops with older ages can be observed at the hills surrounding the basin [22]. Numerous geotechnical investigations including in situ and laboratory studies were carried out in the Duzce basin at different periods following the 1999 Duzce earthquake to determine the geotechnical site conditions. The in situ and laboratory test results indicated that the surface soil layer within the 20 m depth is a quaternary deposit composed of low plasticity silty clay with sand. For this layer, the liquid limit (LL) and plasticity index (PI) values vary between 30–50 and 10–25%, respectively. The standard penetration test blow counts (SPT-N) in this layer mostly range between 5 and 15. Below the surface layer, an alluvial deposit consisting of medium to stiff low plasticity silt, silty–clayey sand and medium dense–dense gravel with cobbles exists. The size of the soil grains in this deposit got coarser with respect to increasing depth. The ground water depth at the basin had a range between 4 and 10 m.

3 Microtremor Survey and Basin Edge Model

A microtremor survey was performed at Duzce basin in order to evaluate the deep subsurface structure and estimate the shear wave velocity profile, which were used to constitute the edge model. The microtremor measurements were taken in order to ensure the most favorable conditions during measurements so that the three-component velocity meter sensors were installed to prevent soil-sensor coupling and reduce the adverse effects that could arise from nearby structures, transient and monochromatic motion sources. During measurements, the data were recorded in accordance with the requirements of reliability for a microtremor survey [23]. The duration of the recordings was selected as 15 min for each measurement point, and the sampling frequency of the records was 100 Hz. During the data processing stage, these recordings were divided into separate windows of 81.92-s duration and every data window was checked to identify whether it had been affected by transient or monochromatic noise sources or not. After excluding artificial disturbances, the Fourier spectra of the segments were calculated by fast Fourier transform method and smoothing process was applied. Next, E–W and N–S horizontal spectra components were merged by taking their geometrical mean. Finally, H/V spectral ratio for each individual window was calculated and the average H/V spectral ratios were obtained [24,25].

Single-point microtremor measurements were taken at 25 different points in the basin along a line from the south to the north as shown in Fig. 2. The ratio of horizontal spectrum to vertical spectrum is related to Rayleigh wave ellipticity; thus, H/V ratios of microtremor data were used to determine shallow subsurface structure. The thickness value for each top layer was estimated by providing the best fit between the H/V curve and theoretical Rayleigh wave ellipticity [26]. During this process, the shear wave profile obtained from the microtremor array measurements was used as a reference model following the suggestions of Yamanaka and Ishida [27].

Furthermore, peak periods of the H/V spectra were fitted carefully. Some examples of the H/V spectra comparison with the theoretical ellipticity of Rayleigh waves are shown in Fig. 2. The thicknesses of the top layers at the microtremor measurement sites were calculated to be varying between 20 and 40 m with an average shear wave velocity value of 245 m/s.

According to the microtremor measurements, it was assumed that the basin was composed of seven separate layers with different shear wave velocities. The layer with a shear wave velocity greater than 800 m/s was considered as seismic bedrock in the basin. The depth of seismic bedrock was estimated by the microtremor array measurements conducted by Kudo et al. [28]. The shear wave velocity profile of the Duzce basin is shown in Fig. 3.

The marked section at the left side of Fig. 3 indicates the edge part of the flat sedimentary basin which was used to build the finite element model in this study. In order to investigate the basin edge effect on the dynamic response of soil layers, edge of Duzce basin was simplified and idealized as given in Fig. 4. After considering the 2D shear wave velocity profile at the basin edge, it was assumed that the seismic bedrock is extending away from its outcrop with a slope value of 1:10 ($\alpha \cong 6°$) (Fig. 3). While creating the basin edge model used in dynamic analyses, soil layers were assumed to extend horizontally within 3 km from the basin edge. In addition, the value of 60 m was taken as the starting depth of the soft rock at the basin edge. In Fig. 4, D is basin depth, X is the distance of a surface point from the beginning of rock outcrop at basin edge, and H is the width of the inclined bedrock at basin edge.

In this study, first the effect of November 12, 1999, Duzce earthquake bedrock ground motion on the two-dimensional dynamic behavior of Duzce basin edge model was examined. The N–S component of the seismic bedrock acceleration time history of the 1999 Duzce earthquake was derived from 1D deconvolution analysis. Afterward, the 2D finite element model was re-analyzed by using different accelerograms and edge slope values to generalize the effects of the change in

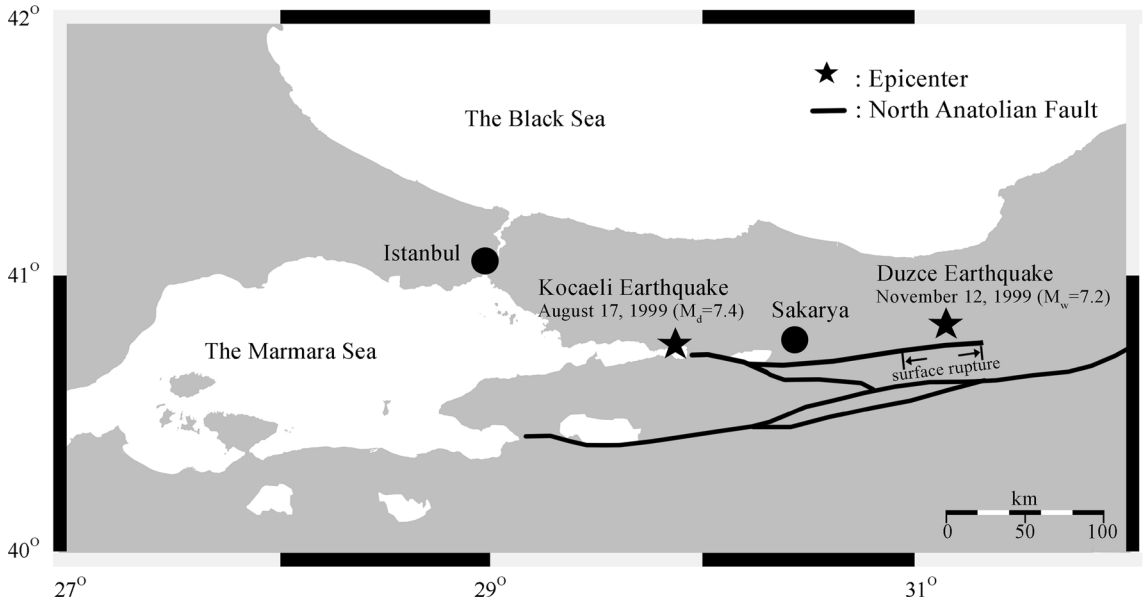

Fig. 1 Location of Duzce, earthquake epicenters and fault system

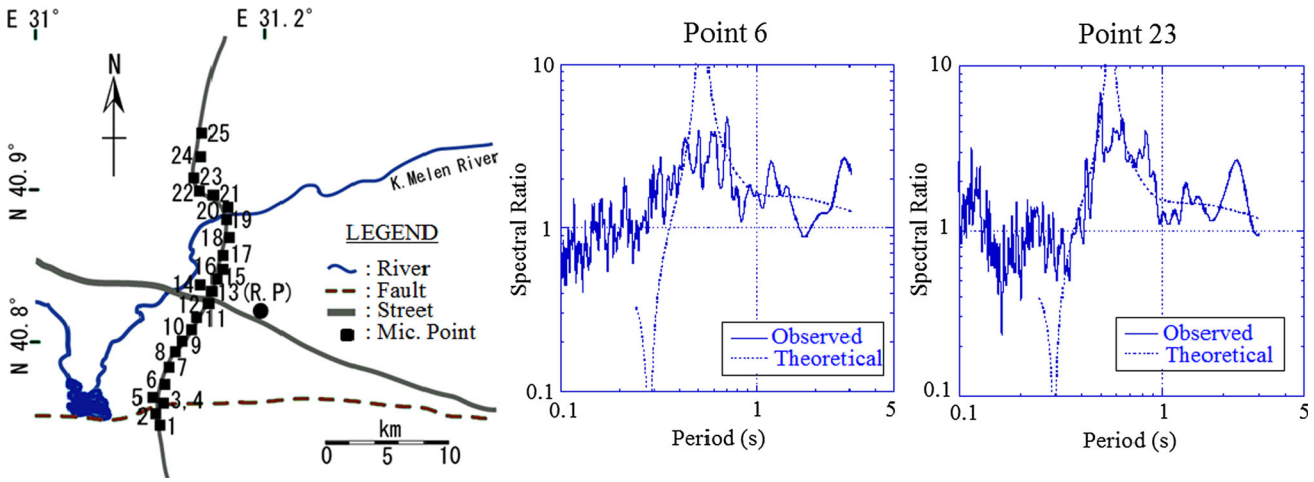

Fig. 2 Locations of single-point microtremor measurements in Duzce basin and comparison of microtremor H/V with calculated ellipticity of Rayleigh waves [25]

strong ground motion intensity levels and basin edge geometry. For this reason, 1D and 2D dynamic analyses were carried out on basin edge models that had been set up with different bedrock inclination values and the results were compared. The basin edge angle values (α) were selected to be in the range of 6°–45° (H/D = 10–1). The depth of the basin (D) was kept constant as 200 m, while the width of basin edge (H) changed between 200 and 2000 m depending on the H/D ratio.

4 Characteristics of the Accelerograms used in the Dynamic Analyses

In order to determine the effects of change in the strong ground motion intensity and frequency content on the seismic response of the basin edge model, six separate accelerograms including both of the rock outcrop and seismic bedrock ground motion data were used for the dynamic analyses of the two-dimensional basin edge models. Two of these strong ground motion accelerograms had been recorded at the San Andreas Fault in North America, which has similar characteristics with the North Anatolian Fault Zone located in Turkey. The rest of the strong ground motion records belong to Turkey earthquakes, and they reflect the characteristics of the different seismotectonical regions of Turkey. Two of these acceleration time histories had been recorded in the building of Sakarya Public Works and Settlement Directorate, including the August 17, 1999, Kocaeli and November 11, 1999, Sakarya earthquakes, respectively. The rest were obtained by the deconvolution of the E–W component of October 1,

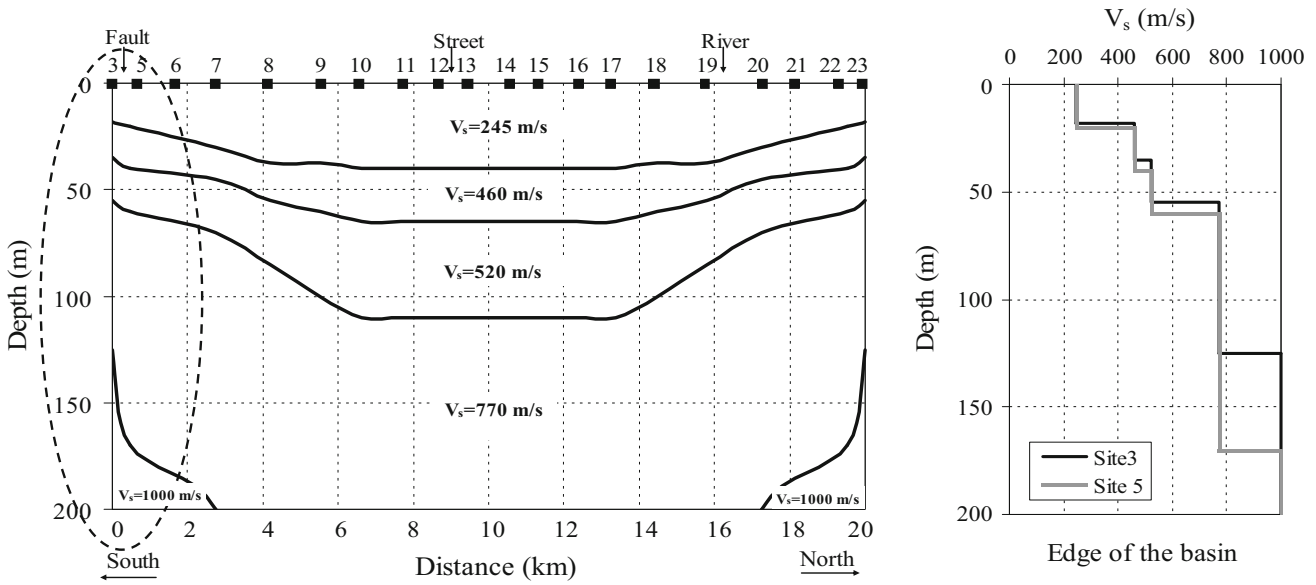

Fig. 3 2D shear wave velocity profile of the Duzce basin

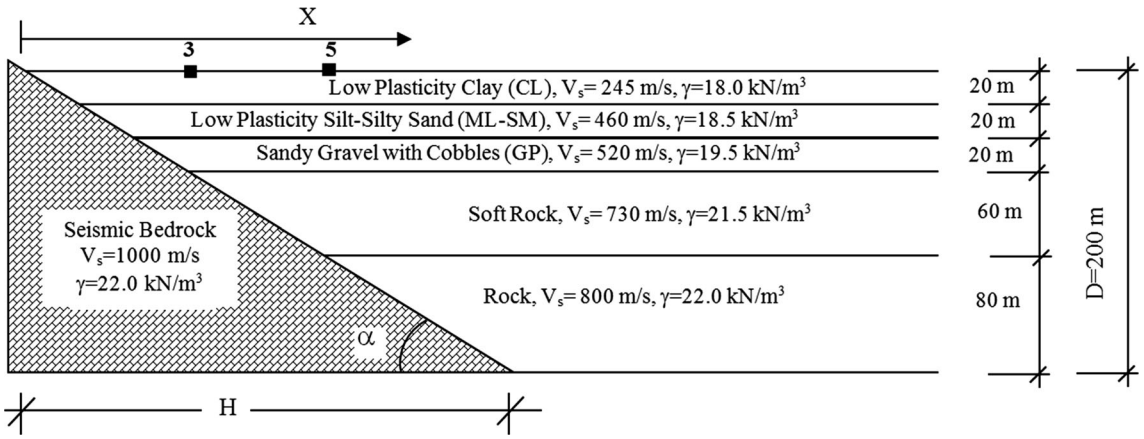

Fig. 4 Idealized basin edge model and soil profile used in the seismic response analyses

1995, Dinar earthquake meteorological station record and N–S component of November 12, 1999, Duzce earthquake meteorological station record. The strong ground motion data used in the dynamic analyses were band-pass-filtered between 0.10 and 25 Hz, and linear baseline corrections were applied. These strong ground motion accelerograms were rescaled to have peak acceleration values (a_{max}) varying between 0.10 and 0.40 g. The rescaling procedure was done by following the recommendation of Krinitszky and Chang [29] which states that the ratio of the target amplitude to the amplitude of the record being scaled should be kept as close to 1 as possible. The rescaled strong ground motion data have different intensity levels and frequency content (v_{max}/a_{max} = 0.03–0.21). The acceleration time histories of the input rock motions and their acceleration spectra are plotted in Figs. 5 and 6, respectively. The general characteristics of the strong ground motion data used in this study are given in Table 1.

5 Methods used in Seismic Response Analyses

The numerical methods developed for the evaluation of dynamic behavior of soil layers against the seismic excitation are defined as 1D, 2D and 3D with respect to the requirements of the problem considered [30]. In general, 1D numerical method is preferred due to the simplicity of its theoretical background and ease of use. On the other hand, while studying with 2D dynamic analysis methods, two-dimensional geometry, shear wave velocity profile and boundary conditions are required for setting up the model and more knowledge is needed to post-process and discuss the analysis results. In this study, Dyneq [31] and Quake/W [32] software that are based on the equivalent linear method

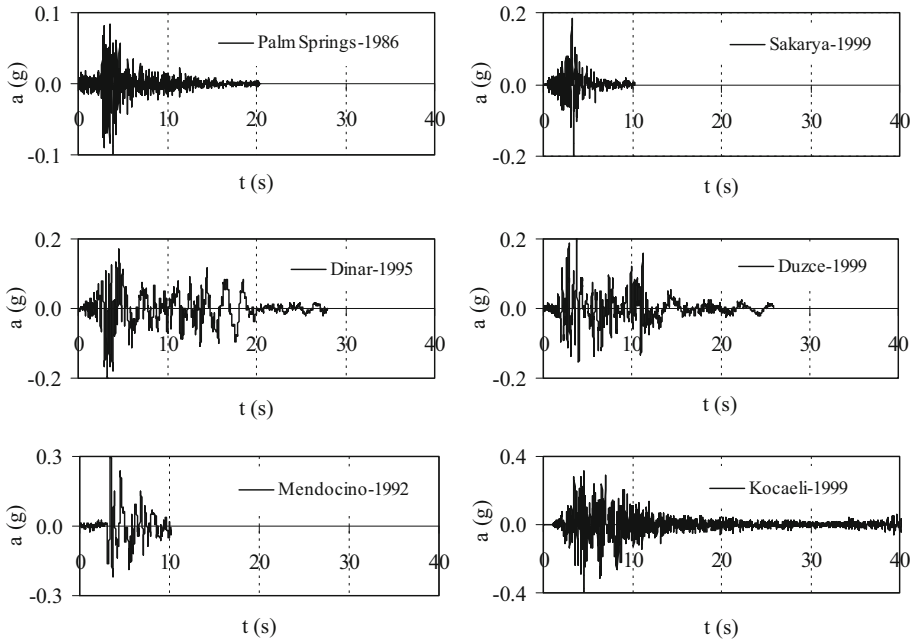

Fig. 5 The acceleration time histories used in the seismic response analyses

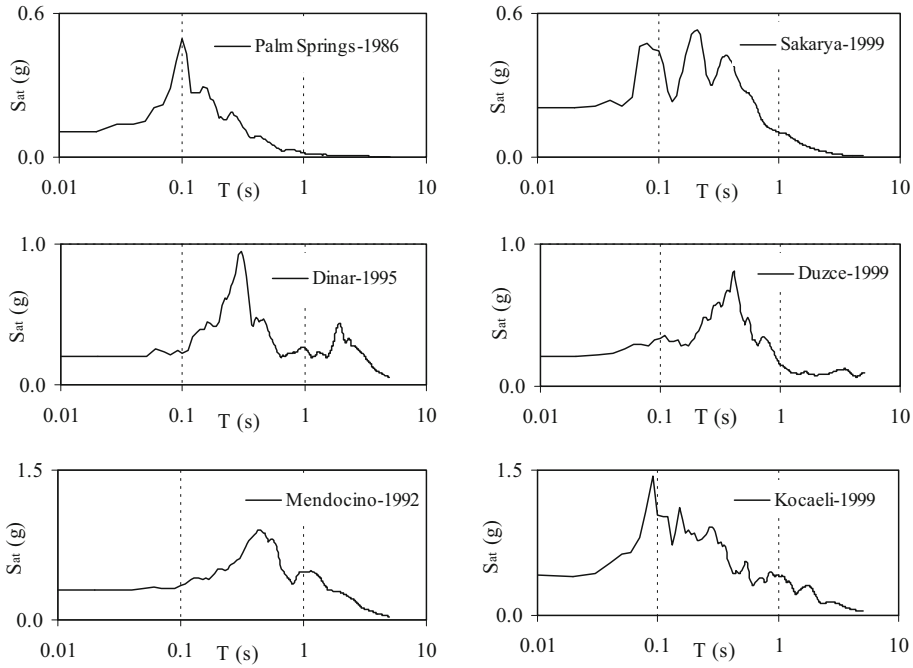

Fig. 6 The acceleration spectra of the input ground motions

were used during the execution of 1D and 2D dynamic analyses, respectively. The properties of soil layers such as soil type, thickness, unit weight and shear wave velocity were obtained from the geotechnical investigations and seismic in situ tests.

The actual nonlinear hysteretic stress–strain behavior of cyclically loaded soils can be approximated by using equivalent linear method. Equivalent linear soil properties such as secant shear modulus (G) and damping ratio (ξ) are strain dependent. In this study, the stiffness degradation of the soil layers with cyclic shear strain (γ_c) was empirically modeled by using Ishibashi–Zhang [33] relation in which the effects of effective confining stress and plasticity index (PI) on shear modulus reduction behavior were combined. The variation in the damping ratio (ξ) of the soil layers with cyclic shear strain (γ_c) was also computed with Ishibashi–Zhang [33] relation. Thus, modulus reduction and damping behavior under cyclic loading were considered for both of the plastic and nonplastic soil layers. For the rock layer lying at the transition zone between soil layers and seismic bedrock, the variation of the dynamic properties with cyclic shear strain was modeled by using the data given by Schnabel et al. [34]. The damping

Table 1 General characteristics of the strong ground motion data used in the dynamic analyses

Earthquake	Palm Springs USA, 1986	Mendocino USA, 1992	Dinar TR, 1995	Kocaeli TR, 1999	Sakarya TR, 1999	Duzce TR, 1999
Record Station	Silent Valley	Cape Petrolia	Dinar Station	Sakarya Sta.	Sakarya Sta.	Duzce Station
Formation	Granite	Rock outcrop	Alluvial	Sandstone	Sandstone	Alluvial
Magnitude	$M_L = 5.9$	$M_L = 6.5$	$M_L = 5.9$	$M_d = 7.4$	$M_d = 5.7$	$M_w = 7.2$
Depth (km)	11.1	14.6	12.0	18.0	8.9	14.0
Epicenter (km)	19.5	15.0	2.0	35.0	17.5	13.0
a_{max} (g)	0.10	0.30	0.20	0.40	0.20	0.20
v_{max} (cm/s)	2.7	36.7	34.8	36.5	13.8	30.7
d_{max} (cm)	3.0	14.2	17.1	16.3	1.6	22.1
I_a (m/s)	0.07	0.82	0.82	1.72	0.14	0.55
CAV (cm/s)	164.2	474.6	818.3	1161.0	166.9	606.4
VSI (cm)	10.3	166.3	142.3	134.1	40.4	64.1
ASI (cm/s)	58.0	254.4	214.8	286.5	147.1	225.0
SMA (cm/s^2)	41.4	217.5	167.4	286.3	103.0	157.0
Location of input motion	Rock outcrop	Rock outcrop	Seismic bedrock	Rock outcrop	Rock outcrop	Seismic bedrock

a_{max} maximum acceleration, v_{max} maximum velocity, d_{max} maximum displacement, I_a arias intensity, CAV cumulative absolute velocity, VSI velocity spectrum intensity, ASI acceleration spectrum intensity, SMA sustained maximum acceleration, TR Turkey

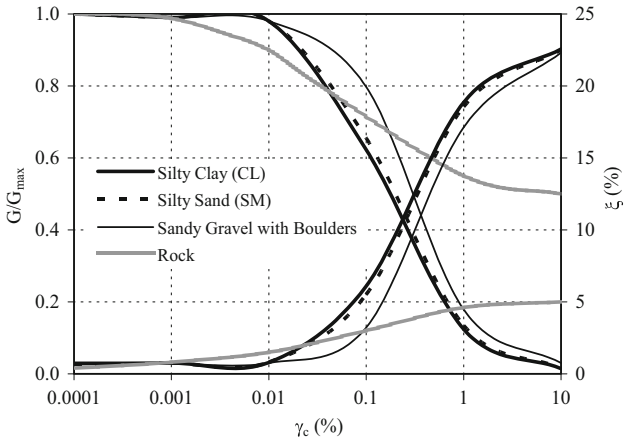

Fig. 7 Normalized shear modulus and damping ratio of the soil layers versus shear strain

ratio of the seismic bedrock was taken as $\xi = 1\%$ and kept constant. The stiffness degradation and damping ratio curves used in the 1D and 2D seismic response analyses are shown in Fig. 7.

5.1 One-dimensional dynamic analysis method

1D dynamic analysis software, Dyneq [31], was used in order to assess the one-dimensional dynamic response of soil layers against the earthquake excitations. Dyneq is a computer code generated for the seismic response analysis of soil layers, which is based on the equivalent linear method and multiple reflection theory. In 1D approximation, the ground motion in any layer can be estimated by using one-dimensional wave propagation theory in layered media. Briefly, this method is based on the calculation of surface motion by the inversion process of the Fourier series of the ground surface (output) motion, which can be defined as the product of the transfer function of layered soil deposits and the Fourier series of bedrock (input) motion.

5.2 Two-dimensional dynamic analysis method

2D dynamic analyses are generally performed by using numerical methods such as finite difference, finite element or hybrid methods. In the finite difference method, a uniform mesh is generally used for modeling the seismic wave propagation in an elastic media. Finite difference method is simple and easy to apply but does not yield satisfactory results while simulating the complex boundary conditions such as surface topography, subsurface geometry and inclined bedrock [35]. The finite element method allows use of irregular mesh with elements having different sizes and geometries to be used; therefore, it is very useful for modeling complex geometry and boundary conditions [36]. There are numerous studies in the literature which examine the effect of soil nonlinearity on seismic response of basins and valleys. Equivalent linear or nonlinear material models have been extensively used in those numerical analyses [4,37–41]. In this study, Quake/W software [32], which is based on the equivalent linear method, was used to carry out the 2D dynamic analyses. The numerical code of this software has a finite element approach.

During the execution of dynamic analyses by Quake/W, the maximum value of normalized nodal displacements (U_{max}) is calculated and compared with the values obtained

from preceding iteration. In equivalent linear method, the calculations will continue until either the user-defined iteration number is reached or the difference between normalized displacements falls under a predetermined convergence (δ_T) value as defined below. $U_{max(i)}$ is the normalized maximum displacement at ith iteration.

$$\delta U_{max} = \left(\text{ABS} \left(U_{max(i+1)} - U_{max(i)} \right) / U_{max(i)} \right) < \delta_T \quad (1)$$

While performing dynamic analyses with Quake/W, the absorbent effect of soil layers and the bedrock lying at the vertical and horizontal boundaries of the finite element model can be taken into account by placing viscous dashpots at those boundaries. Dashpot coefficients are proportional with the pressure and shear wave velocities of the relevant soil layers at the boundaries of the two-dimensional model [42,43].

5.3 Finite Element Model of the Basin and Its Boundary Conditions

The 2D geometry, finite element mesh and boundary conditions of the basin edge model are illustrated in Fig. 8. In this figure, D is the depth of the flat sedimentary basin, H is the width of the inclined bedrock, and X refers to the distance of a surface point from the beginning of rock outcrop at basin edge. Soil profile was divided into 20 different layers with thicknesses of 10 m as shown in the figure. The shear wave velocity of the surface layer and the seismic bedrock was assumed to be approximately 200 and 1000 m/s, respectively.

The appropriate definition of boundary conditions is very important in 2D dynamic analyses. In order to simulate a half-space through a finite element mesh, artificial boundaries can be adopted at each side of the model to reduce the effects of wave reflections and absorb the scattered energy. In a 2D dynamic analysis, it is preferred to put viscous dashpots at the boundaries of the finite element model to emit the energy of both pressure and shear waves; thus, reflection of seismic waves at the boundaries can be diminished [18]. In the case of a fixed base in both directions, the soil amplifications at the surface layers reach unrealistic values, especially when the soil layers show nonlinear behavior in 2D dynamic analyses. Therefore, viscous dashpots having values proportional to shear and pressure wave velocity of soil layers were placed at the vertical and horizontal boundaries of the 2D model. The effect of 1D free field motion was added to the model by applying time-dependent stress functions to both of the vertical boundaries. The boundary forces were calculated by multiplying the 1D particle velocity values of the soil layers with the relevant horizontal dashpot coefficients and then applying them to the 2D model at the boundaries as stress functions changing throughout the earthquake ground motion.

The dynamic analyses were executed in the time domain by Quake/W software [32]. Plane strain elements were used to set up the finite element mesh of the basin edge model. The plane strain finite elements used in the dynamic analyses were quadrilateral and triangular, having 8 and 6 nodes, respectively. In finite element modeling, the accuracy of the numerical results and the computational time depends on the mesh geometry. Thus, the model discretization represents a crucial step of the analysis. In order to avoid the effect of filtering out high-frequency components of the seismic motion, the height, h, of each element in the mesh was selected to meet the following condition:

$$h \leq \left(\frac{1}{5} \right) \frac{V_s}{f_{max}} \quad (2)$$

where V_s is the shear wave velocity of the element and f_{max} is the maximum frequency of the input motion. Moreover, to ensure accurate numerical solutions, the width l of each element was selected according to the condition $l \leq 5h$.

6 Results of Two-Dimensional Dynamic Analyses

Two-dimensional dynamic analyses were performed by using the model shown in Fig. 8 to study the effect of basin edge inclination on soil amplification. The horizontal acceleration time histories and their maximum values were calculated for different sections of the flat sedimentary basin surface by using separate input rock motions. The maximum absolute surface acceleration values (a_{max_s}) were normalized by dividing them with the maximum absolute acceleration values of the rock outcrop motion (a_{max_r}); thus, 2D soil amplifications ($A = a_{max\_s}/a_{max\_r}$) were calculated for the flat sedimentary basin models with different edge slope values. The variation of the 2D soil amplification values with the dimensionless distance (X/D) and edge bedrock inclination values ($H/D = 10, 5, 2, 1$) is shown in Fig. 9 for different input rock motions. As illustrated in the figure, initially 2D soil amplifications reached their peak values at definite sections of the basin surface with increasing distance from the edge and afterward for every different acceleration time history, they mostly converged with the increase in X/D values regardless of the bedrock inclination value. From Fig. 9, it can be observed that a limited edge section with an approximate width of 2.5 D is influenced by basin edge effect, while the other parts of the basin have nearly the same amplification levels. This finding is consistent with the numerical results of the other studies presented in the literature such as Gelagoti et al. [41,44], Khanbabazadeh and Iyisan [4], Hasal and Iyisan [19] and Riga [45].

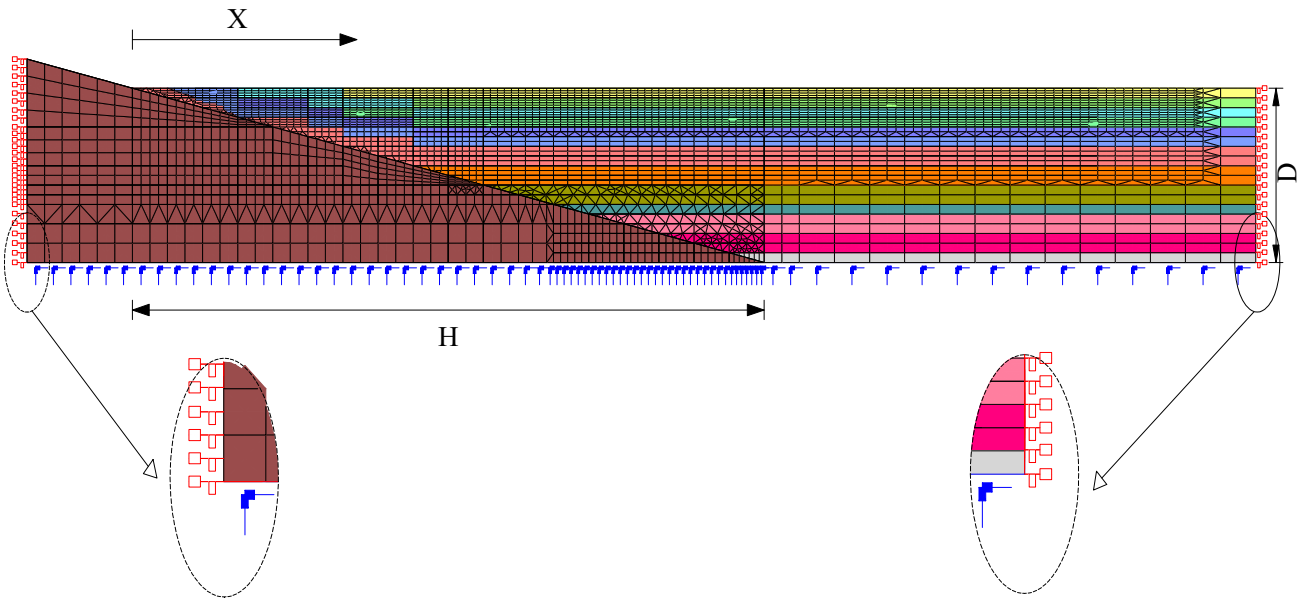

Fig. 8 2D basin edge model, its finite element mesh and boundary conditions

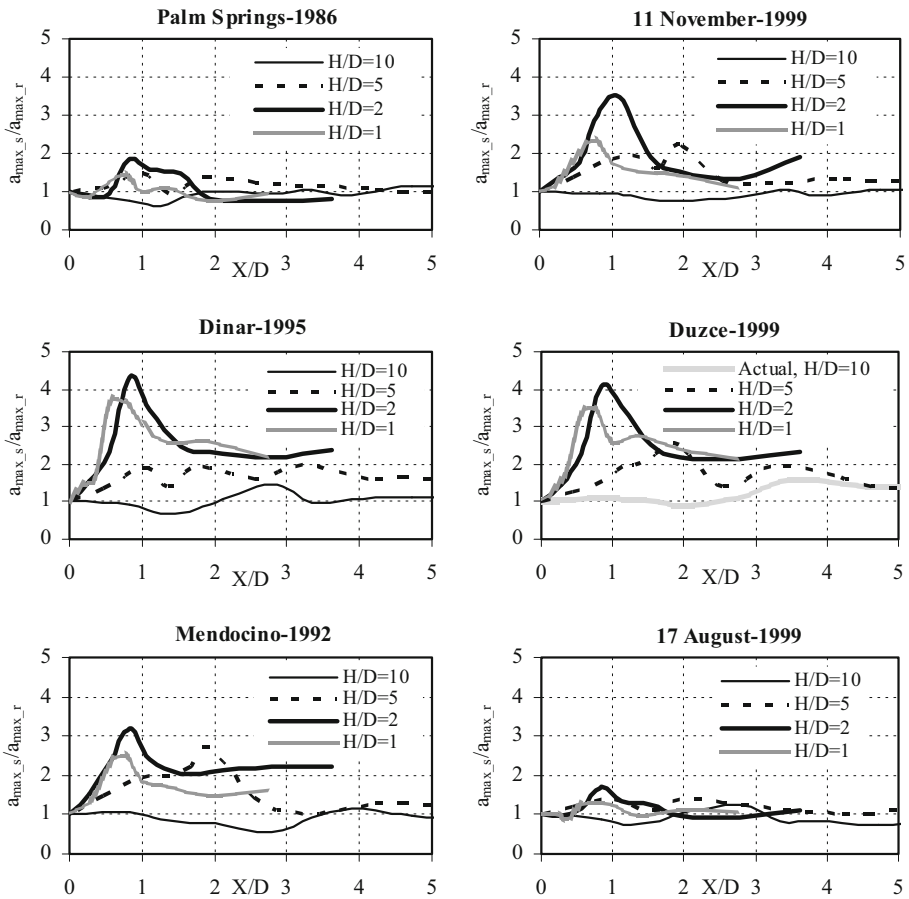

Fig. 9 The variation of the soil amplification values calculated at the basin edge model for different input rock motions and varying edge inclination values

The computed soil amplification values at basin edges were remarkably higher for the edge models with steep slopes ($H/D = 2, 1$) in comparison with the models with gentle slopes ($H/D = 10, 5$). The frequency content of the input rock motion had a strong effect on the 2D soil amplification values, especially for the basin edges with steep slope values

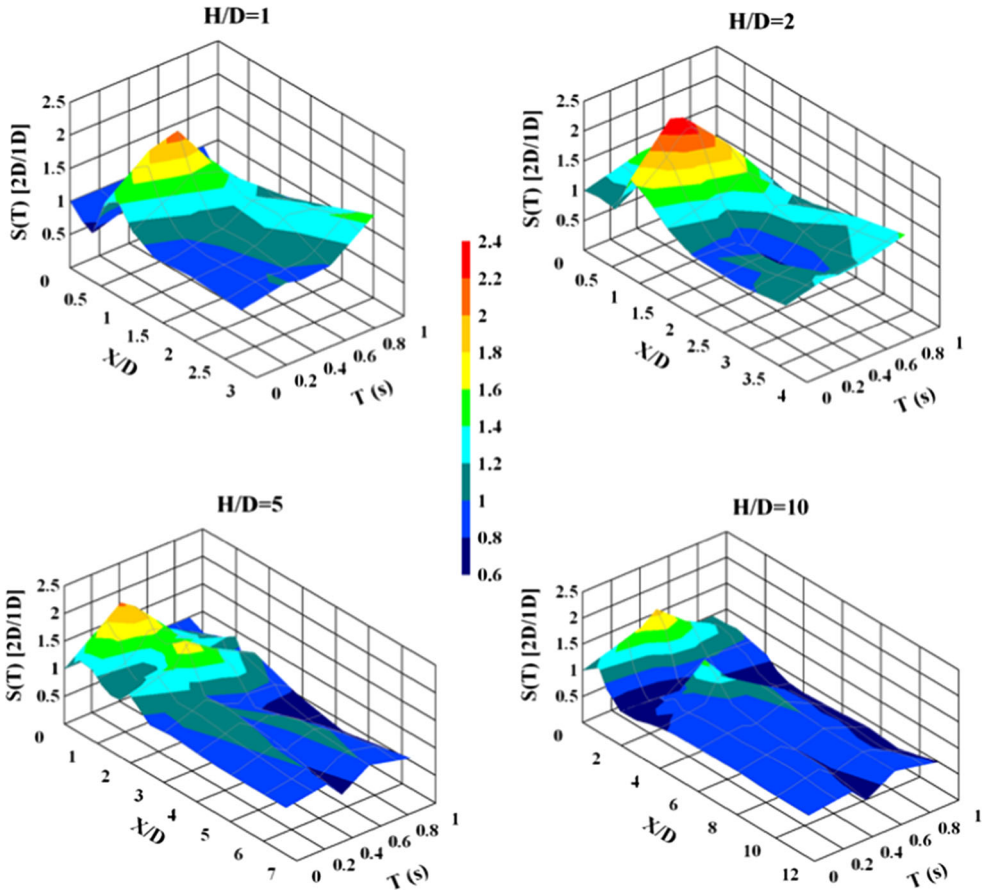

Fig. 10 The variation of aggravation factors with X/D and period values

($H/D = 2, 1$). For 1995 Dinar and 1999 Duzce earthquake input rock motions, 2D soil amplifications took values as high as 4.0 at basin edge section, $X/D = 1$, while amplification values less than 2.0 were calculated for some of the other input motions. The calculated soil amplifications generally took values between 1.0 and 2.0 for the basin edge models with gentle slope values ($H/D = 5, 10$). The variation of the computed amplification values along the actual edge of Duzce basin ($H/D = 10$) is depicted in Fig. 9. As the edge slope values became lower ($H/D \leq 10$), 2D soil amplification values generally approached to 1 regardless of the input rock motion frequency content.

7 Comparison of 1D and 2D Dynamic Analyses

The difference between 1D and 2D dynamic behaviors was studied for the edge section of flat sedimentary basin models by comparing the acceleration response spectra obtained from the seismic response analyses. The ratio of the spectral accelerations that is calculated from the results of 2D and 1D dynamic analyses is defined as spectral acceleration ratio–aggravation factor [46]. Aggravation factor can also be expressed as the additional amplification of a 2D model to its corresponding 1D model, and it can be used to reflect the effect of lateral boundary on the 1D spectral acceleration values estimated for different points at basin edge section.

The aggravation factors were calculated for different period values at separate basin models with different edge slope values in order to investigate the effects of change in edge bedrock inclination on the frequency content of the earthquake excitation. The variation of the average values of aggravation factors is shown in Fig. 10 as three-dimensional surface plots for flat sedimentary basin models with different edge slope values ($H/D = 1$, $H/D = 2$, $H/D = 5$ and $H/D = 10$).

As it is depicted in Fig. 10, aggravation factors reached their peak values at a definite zone on the basin edge and they nearly became equal to 1 for different period values while approaching to the middle part of the basin. It can also be concluded that the aggravation factor values became closer to each other after a specific value of X/D term ($X/D = 3$) regardless of the edge bedrock inclination value. Although the aggravation factors took peak values varying between 2.0 and 2.5 for the cases of $H/D = 5$, 2 and 1 (α=11°, 27° and 45°), the increase in aggravation factor values became most

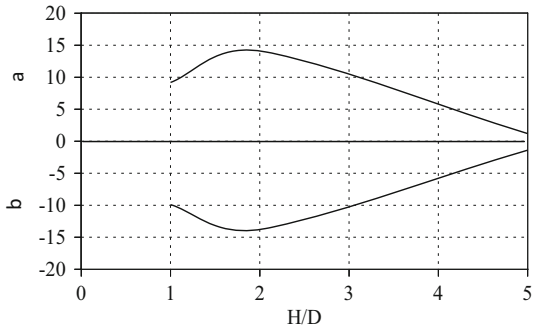

Fig. 11 The variation of a and b parameters with the edge inclination value

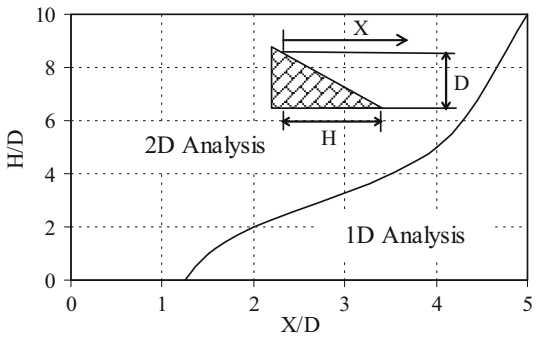

Fig. 12 The limit of validity of the 1D seismic response analysis at the basin edge as a function of the bedrock inclination and of the distance from rock outcrop

noticeable when H/D was equal to 2 (α=27°). Likewise, the aggravation factor reached a peak value higher than 2.0 in the study of Chavez-Garcia and Faccioli [47]. In the Euroseistest case, the aggravation factor took peak value of 5.0 for periods larger than 0.3 s [46]. Iyisan and Khanbabazadeh [48] obtained maximum aggravation factor values varying between 0.55 and 2.0 in their study, and they pointed out that the aggravation factor values depend on input motion amplitude as well as soil type. Riga [45] suggested three different aggravation factor values as 1.1, 1.2 and 1.9 to be used for different site classifications and periods.

In this study, an attempt was made to define the variation of the average values of aggravation factors by a unique function and/or constant value for each edge bedrock slope and period value. The aggravation factor curves obtained for different basin edge geometry were clearly nonlinear, and they had extremely high and low values more than 1; thus, it was necessary to idealize the curves by using a function that is dependent on the distance from rock outcrop, depth of basin and edge slope value. The variation of the average aggravation factor at basin edge with the distance from the bedrock outcrop was defined as given below for the flat sedimentary basin models on condition that $X/D>0$:

$$S(T)\,[2D/1D] = e^{\left(a+\frac{b}{(X/D)}+b\ln\frac{X}{D}\right)} + 1 \tag{3}$$

In this equation, the aggravation factor is shown by $S(T)$[2D/1D]. X and D indicate the distance from the rock outcrop at basin edge and the total depth of soil deposit and soft rock lying over seismic bedrock, respectively. Also a and b represent the parameters that are dependent on the edge slope and period values. For the case of $H/D = 2$, the aggravation factors reached their maximum values, especially at $T = 0.3$–0.5 s period interval for which the difference between 1D and 2D dynamic behaviors became very remarkable and the parameters, a and b, took approximate values of 14 and -14, respectively (Fig. 11).

Regardless of the period values, the average aggravation factor values approached to 1 after the point of $X/D =$ 5, 4, 2, 1.5 for the models with $H/D = 10, 5, 2, 1$, respectively. After these points, two-dimensional effects decreased significantly. Using this result, the limits of the basin edge sections where 2D dynamic behavior should be taken into account can be obtained. In Fig. 12, the validity limits of 1D and 2D dynamic analysis at the basin edge are illustrated for different H/D and X/D values.

The aggravation factor relationship given in Eq. 3 was proposed for the edge section of a flat sedimentary basin model, which was constituted by using the data obtained from in situ measurements that had been carried out by the authors. However, it can be calibrated for other soil conditions by modifying the values of the parameters given in Eq. 3 [16,19].

8 Discussion on the Results of Aggravation Factor Calculations

For all the basin edge models, the aggravation factors reached their highest values when the periods were between 0.2 and 0.6 s. The aggravation factors became considerably smaller with the decrease in edge inclination values. The exponential function given in Eq. 3 was considered to be successful in representing the zones where the aggravation factor curves reached their peak values; however, it could not simulate the behavior of some aggravation factor curves that had fluctuations. Nevertheless, it is assumed that the fluctuating behavior in aggravation factor values, which was recognized close to rock outcrop at the edges of some models, may not come into existence perfectly in nature since the soil layers at basin edges are usually stiffer or denser in comparison with the sedimentary formations lying at middle sections of basin surface. The stiffer layers at the basin edges can be classified as talus and residual soil that are formed by accumulation of rock fragments at the base of cliffs and chemical/physical weathering of native bedrock in place, respectively. It can be speculated that these stiffer soil layers will show a softening behavior on the fluctuations observed in aggravation factor

curves since they provide a lessening effect in the impedance contrast between edge seismic bedrock and overlying soil layers in comparison with the idealized horizontally layered basin edge models. For this reason, the secondary increments and decrements that had been obtained in the values of aggravation factor curves for the zones of alluvium located close to the rock outcrop were neglected. It was also observed that for some basin models and period values, the aggravation factors took constant values between 0.7 and 1.3 at the basin edges.

9 Conclusions

In this study, the effect of basin edge inclination on the variation of surface ground motion was investigated for different earthquake excitations. The shear wave velocity profile of the basin edge models was generated by using the data obtained from the in situ measurements that had been carried out at Duzce basin located in Turkey, and the seismic responses at edge sections of the flat sedimentary basin models were computed. The changes in the soil amplification and 2D/1D aggravation factor values with the distance from the basin edge were calculated by one- and two-dimensional dynamic analyses, and the results were compared. A relationship between the aggravation factor value and basin edge geometry was developed. The findings and contributions obtained in this study can be summarized as given below.

The maximum increments in soil amplification values occurred between rock outcrop and the point $X/D = 3$ for all of the basin edge models used in the analyses. Also the aggravation factors reached their maximum values at a definite section ($X/D<3$) of basin edge for every interested period value. The aggravation factors took average values between 0.6 and 2.5 for different input ground motion data. With increasing distance from the basin edge, especially after the point $X/D = 3$, the aggravation factor values mostly approached to 1 regardless of the edge inclination and period values.

The effect of seismic bedrock inclination on the seismic response of soil layers located at basin edges was studied, and the maximum aggravation factor values were calculated for the case of $H/D = 2$.

For all the basin models with different edge geometry, the aggravation factors reached their peak values for the periods between 0.2 and 0.6 s. The average aggravation factors took values varying between 2.0 and 2.5 at the period interval of 0.2–0.5 s for the basin models with $H/D = 2$. With the decrease in edge bedrock slope value ($H/D = 10$, $\alpha=6°$), the difference between 1D and 2D spectral acceleration values noticeably decreased.

For the basin models with H/D values of 10, 5, 2 and 1, the average aggravation factors approached to 1 for X/D values greater than 5, 4, 2 and 1.5, respectively. It was assumed that the two-dimensional effects can be neglected beyond these points.

The aggravation factor relation proposed in this study can be considered useful in reflecting the second dimension effect to the spectral acceleration value calculated from 1D seismic site response analysis, depending on edge bedrock inclination value and X/D dimensionless term. It is possible to modify this equation for different geotechnical site conditions by using the findings obtained from future research.

References

1. Lacave, C.; Bard, P.Y.; Koller, M.G.: Microzonation: techniques and examples. In: Block 15: Naturgefahren-Erdbebenrisiko. p. 23 (1999). http://citeseerx.ist.psu.edu/viewdoc/download?doi=10.1.1.491.9369&rep=rep1&type=pdf
2. Gallipoli, M.R.; Bianca, M.; Mucciarelli, M.; Parolai, S.; Picozzi, M.: Topographic versus stratigraphic amplification: mismatch between code provisions and observations during the L'Aquila (Italy, 2009) sequence. Bull. Earthq. Eng. **11**(5), 1325–1336 (2013)
3. Iyisan, R.; Hasal, M.E.: The effect of ground motion characteristics to the dynamic response of alluvial valley models. In: 13th Asian Regional Conference of Soil & Geotechnical Engineering, Theme-7 Dam Engineering, Paper Code 7.1-8, Kolkata, India (2007)
4. Khanbabazadeh, H.; Iyisan, R.: A numerical study on the 2D behavior of the clayey basins. Soil Dyn. Earthq. Eng. **66**, 31–41 (2014)
5. Pitilakis, K.: Site effects. In: Ansal, A. (ed.) Recent Advances in Earthquake Geotechnical Engineering and Microzonation, vol. 1, pp. 139–193. Kluwer Academic Publishers, Dordrecht (2004)
6. Rassem, M.; Ghobarah, A.; Heidebrecht, A.C.: Engineering perspective for the seismic site response of alluvial valleys. Earthq. Eng. Struct. Dyn. **26**, 477–493 (1997)
7. Ohtsuki, A.; Yamahara, H.; Tazoh, T.: Effect of lateral inhomogeneity on seismic waves, II: observation and analysis. Earthq. Eng. Struct. Dyn. **12**, 795–816 (1984)
8. Gazetas, G.; Fan, K.; Tazoh, T.; Shimizu, K.: Seismic response of the pile foundation of Ohba Ohashi Bridge. In: Proceedings of the 3rd International Conference on Case History in Geotechnical Engineering, pp. 1803–1809 (1993)
9. Chavez-Garcia, F.J.; Rodriguez, M.; Stephenson, W.R.: 1D vs. 2D site effects: the case of Parkway Basin, New Zealand. In: 11th European Conference on Earthquake Engineering, Balkema, Rotterdam (1998)
10. Field, E.H.: Spectral amplification in a sediment-filled valley exhibiting clear basin edge induced waves. Bull. Seismol. Soc. Am. **86**, 991–1005 (1996)
11. Raptakis, D.; Chavez-Garcia, F.J.; Makra, K.; Pitilakis, K.: Site effects at Euroseistest—I: determination of the valley structure and confrontation of observations with 1D analysis. Soil Dyn. Earthq. Eng. **19**(1), 1–22 (2000)
12. Makra, K.; Chavez-Garcia, F.J.; Raptakis, D.; Pitilakis, K.: Parametric analysis of the seismic response of a 2D sedimentary valley: implications for code implementations of complex site effects. Soil Dyn. Earthq. Eng. **25**(4), 303–315 (2005)
13. Semblat, J.F.; Dangla, P.; Kham, M.: Seismic site effects for shallow and deep alluvial basins: in-depth motion and focusing effect. Soil Dyn. Earthq. Eng. **22**, 849–854 (2002)
14. Gelagoti, F.; Kourkoulis, R.; Tsirantonaki, D.; Gazetas, G. 2-dimensional non-linear valley effects at Heathcote Valley during the 2011 Canterbury earthquake: a case study. In: 2nd European Conference on Earthquake Engineering and Seismology, Istanbul, 25–29 Aug 2014

15. Hasal, M.E.; Iyisan, R.: Effect of edge slope on soil amplification at a two dimensional basin model. In: 15th World Conference on Earthquake Engineering, Lisboa, Paper no: 4455 (2012)
16. Iyisan, R.; Hasal, M.E.: The basin edge effect on dynamic response: dinar basin model. IMO Tech. J. Dig. **22**, 1499–1518 (2011)
17. Ciliz, S.; Ozkan, M.Y.; Cetin, K.O.: Effect of basin edge slope on the dynamic response of soil deposits. In: 4 th International Conference on Earthquake Geotechnical Engineering, Thessaloniki, Paper no: 1309 (2007)
18. Hasal, M.E.: The effects of topographical irregularities on soil amplification (in Turkish). Dissertation, PhD Thesis, Istanbul Technical University Institute of Science and Technology (2008)
19. Hasal, M.E.; Iyisan, R.: A numerical study on comparison of 1D and 2D seismic responses of a basin in Turkey. Am. J. Civil Eng. **2**(5), 123–133 (2014). https://doi.org/10.11648/j.ajce.20140205.11
20. Yamanaka, H.: Geophysical Exploration of Sedimentary Structures and Their Characterization. The Effects of Surface Geology on Seismic Motion, pp. 15–33. Balkema, Rotterdam (1998)
21. Barka, A.; Akyuz, H.S.; Altunel, E.: The August 17, 1999 Izmit earthquake, M=7.4, and November 12, 1999 Duzce earthquake, M=7.2, eastern Marmara Sea region. In: Proceedings of the International Conference on Earthquake Hazard and Risk in the Mediterranean Region, Near East University, Lefkosa, vol. 1, pp. 13–22 (1999)
22. Simsek, O.; Dalgic, S.: Consolidation properties of the clays at Duzce plain and their relationship with geological evolution. Geolog. Bull. Turkey **40**(2), 29–38 (1997)
23. SESAME: Guidelines for the implementation of the H/V spectral ratio technique on ambient vibrations: measurements, processing and interpretation. SESAME European Research Project, WP12-Deliverable D23.12, European Commission-Research General Directorate, Project No:EVG1-CT2000-00026 (2004)
24. Ansal, A.; Iyisan, R.; Gullu, H.: Microtremor measurements for the microzonation of Dinar. Pure Appl. Geophys. **158**(12), 2525–2541 (2001)
25. Hasal, M.E.; Iyisan, R.; Khanbabazadeh, H.; Bayin, A.; Cevikbilen, G.; Kepceoglu, O.: A preliminary seismic microzonation study based on microtremor measurements. In: International Conference: Skopje Earthquake-50 years of European Earthquake Engineering, Skopje (2013)
26. Yamanaka, H.; Kato, M.; Hashimoto, M.; Gulerce, U.; Iyisan, R.; Ansal, A.: Microtremor and earthquake observations in Adapazari and Duzce, Turkey, for estimations of site amplifications. In: Proceedings of the Assessment of Seismic Local Site Effects at Plural Test Sites, Ministry of Education, Science, Sports and Culture, Research Grant No: 11694134, Japan, pp. 129–136 (2002)
27. Yamanaka, H.; Ishida, H.: Application of genetic algorithms to an inversion of surface-wave dispersion data. Bull. Seismol. Soc. Am. **86**(2), 436–444 (1996)
28. Kudo, K.; Kanno, T.; Okada, H.; Ozel, O.; Erdik, M.; Sasatani, T.; Higashi, S.; Takahashi, M.; Yoshida, K.: Site-specific issues for strong ground motions during the Kocaeli, Turkey, earthquake of 17 August 1999, as inferred from array observations of microtremors and aftershocks. Bull. Seismol. Soc. Am. **92**(1), 448–465 (2002)
29. Krinitszky, E.L.; Chang, F.K.: State-of-the-art for assessing earthquake hazards in the United States: specifying peak motions for design earthquakes. Miscellaneous Paper S-73-1, Report 7, U.S. Army Corps of Engineers Waterways Experiment Station, Vicksburg, Mississippi (1979)
30. Matasovic, N; Hashash, Y.M.A.: Practices and procedures for site-specific evaluations of earthquake ground motions. NCHRP Synthesis 428, Transportation Research Board, Washington, p. 90 (2012)
31. Yoshida, N.; Suetomi, I.: DYNEQ Manual: A computer program for dynamic response analysis of level ground by equivalent linear method, Version 3.23 (2003)
32. Krahn, J.: Dynamic Modeling with QUAKE/W: An Engineering Methodology. Geo-Slope International, Calgary (2007)
33. Ishibashi, I.; Zhang, X.: Unified dynamic shear moduli and damping ratios of sand and clay. Soils Found. Jpn. Soc. Soil Mech. Found. Eng. **33**(1), 182–191 (1993)
34. Schnabel, P.B.; Lysmer, J.; Seed, H.B.: SHAKE: a computer program for earthquake response analysis of on horizontally layered sites. Report No. UCB/EERC 72-12, p. 102. Earthquake Engineering Research Center, University of California, Berkeley (1972)
35. Aoi, S.; Fujiwara, H.: 3D finite-difference method using discontinuous grids. Bull. Seismol. Soc. Am. **89**, 918–930 (1999)
36. Gatmiri, B.; Arson, C.; Nguyen, K.V.: Seismic site effects by an optimized 2D BE/FE method: theory, numerical optimization and application to topographical irregularities. Soil Dyn. Earthq. Eng. **28**, 632–645 (2008)
37. Pavlenko, O.V.: Nonlinear seismic effects in soils: numerical simulation and study. Bull. Seismol. Soc. Am. **91**(2), 381–396 (2001)
38. Olsen, K.B.; Akinci, A.; Rovelli, A.; Marra, F.; Malagnini, L.: 3D ground motion estimation in Rome, Italy. Bull. Seismol. Soc. Am. **96**(1), 133–146 (2006)
39. Psarropoulos, P.N.; Tazoh, T.; Gazetas, G.; Apostolou, M.: Linear and nonlinear valley amplification effects on seismic ground motion. Soils Found. **47**(5), 857–871 (2007)
40. Lacave, C.; Bard, P.Y.; Kham, M.; Koller, M.G.: 2D equivalent linear site effect simulation: example applications to two deep valleys. Bull. Earthq. Eng. **6**, 197–211 (2008)
41. Gelagoti, F.; Kourkoulis, R.; Anastasopoulos, I.; Gazetas, G.: Nonlinear dimensional analysis of trapezoidal valleys subjected to vertically propagating SV waves. Bull. Seismol. Soc. Am. **102**(3), 999–1017 (2012)
42. Lysmer, J.; Richart, F.E.: Dynamic response of footings to vertical loadings. ASCE J. Soil Mech. Found. Div. **92**(SM1), 65–91 (1966)
43. Lysmer, J.; Kuhlemeyer, R.L.: A finite dynamic model for infinite media. ASCE J. Eng. Mech. Div. **95**(EM4), 859–877 (1969)
44. Gelagoti, F.; Kourkoulis, R.; Anastasopoulos, I.; Tazoh, T.; Gazetas, G.: Seismic wave propagation in a very soft alluvial valley: sensitivity to ground-motion details and soil nonlinearity, and generation of a parasitic vertical component. Bull. Seismol. Soc. Am. **100**(6), 3035–3054 (2010)
45. Riga, E.D.: New elastic spectra, site amplification factors and aggravation factors for complex subsurface geology, towards the improvement of EC8. Dissertation, PhD Thesis, Aristotle University of Thessaloniki, Greece (2015)
46. Makra, K.; Raptakis, D.; Chavez-Garcia, F.J.; Pitilakis, K.: Site effects and design provisions: the case of Euroseistest. J. Pure Appl. Geophys. **158**(12), 2349–2367 (2001)
47. Chavez-Garcia, F.J.; Faccioli, E.: Complex site effects and building codes: making the leap. J. Seismol. **4**, 23–40 (2000)
48. Iyisan, R.; Khanbabazadeh, H.: A numerical study on the basin edge effect on soil amplification. Bull. Earthq. Eng. **11**(5), 1305–1323 (2013)